Luminescent PtII and PtIV Platinacycles with Anticancer Activity Against Multiplatinum-Resistant Metastatic CRC and CRPC Cell Models

Ariadna Lázaro[+,[a]] Cristina Balcells[+,[b]] Josefina Quirante,[c, g] Josefa Badia,[d, g] , Laura Baldomà,[d, g] Jas S. Ward,[f] Kari Rissanen,[f] Mercè Font-Bardia,[e] Laura Rodríguez,[a, h] ,Margarita Crespo,*[a, g] and Marta Cascante*[b, g, i]

[a] A. Lázaro,+ Prof. L. Rodríguez, Dr. M. Crespo
Dpt de Química Inorgànica i Orgànica, Secció de Química Inorgànica
Facultat de Química, Universitat de Barcelona
Martí i Franquès 1–11, 08028 Barcelona (Spain)
E-mail: margarita.crespo@qi.ub.es

[b] C. Balcells,+ Prof. M. Cascante
Dpt. of Biochemistry and Molecular Biomedicine
Faculty of Biology, Universitat de Barcelona
Av. Diagonal, 643, 08028 Barcelona (Spain)
E-mail: martacascante@ub.edu

[c] Dr. J. Quirante
Laboratori de Química Orgànica
Facultat de Farmàcia, Universitat de Barcelona
Av. Joan XXIII, 27–31, 08028 Barcelona (Spain)

[d] Prof. J. Badia, Prof. L. Baldom/
Dpt de Bioquìmica i Fisiologia
Facultat de Farmàcia, Universitat de Barcelona
Av. Joan XXIII, 27–31, 08028 Barcelona (Spain)

[e] Dr. M. Font-Bardia
Unitat de difracciò de RX, CCiTUB, Universitat de Barcelona
Solé i Sabarís 1–3, 08028 Barcelona (Spain)

[f] Dr. J. S. Ward, Prof. K. Rissanen
Dpt of Chemistry, Nanoscience Center, University of Jyvaskyla
P.O. Box 35, Jyvaskyla, 40014 (Finland)

[g] Dr. J. Quirante, Prof. J. Badia, Prof. L. Baldomà, Dr. M. Crespo,
Prof. M. Cascante
Institut de Biomedicina, Universitat de Barcelona (IBUB)
08028 Barcelona (Spain)

[h] Prof. L. Rodríguez
Institut de NanociHncia i Nanotecnologia
Universitat de Barcelona (IN2UB), 08028 Barcelona (Spain)

[i] Prof. M. Cascante
Centro de Investigación Biomèdica en Red de Enfermedades Hepáticas-digestivas,
(CIBEREHD), Instituto de Salud Carlos III (ISCIII), Madrid (Spain)

ABSTRACT:

Platinum-based chemotherapy persists to be the only effective therapeutic option against a wide variety of tumours. Nevertheless, the acquisition of platinum resistance is utterly common, ultimately cornering conventional platinum drugs to only palliative in many patients. Thus, encountering alternatives that are both effective and non-cross-resistant is urgent. In this work, we report the synthesis, reduction studies, and luminescent properties of a series of cyclometallated (C,N,N')PtIV compounds derived from amine–imine ligands, and their remarkable efficacy at the high nanomolar range and complete lack of cross-resistance, as an intrinsic property of the platinacycle, against multiplatinum-resistant colorectal cancer (CRC) and castration-resistant prostate cancer (CRPC) metastatic cell lines generated for this work. We have also determined that the compounds are effective and selective for a broader cancer panel, including breast and lung cancer. Additionally, selected compounds have been further evaluated, finding a shift in their antiproliferative mechanism towards more cytotoxic and less cytostatic than cisplatin against cancer cells, being also able to oxidize cysteine residues and inhibit topoisomerase II, thereby holding great promise as future improved alternatives to conventional platinum drugs.

Platinum-based chemotherapy is often the only effective treatment Against a broad spectrum of tumors, even if their success Is limited by side-effects and resistance. Octahedral ptiv compounds Have been shown to be a very promising kind of prodrugs Since they are kinetically inert compared to ptii analogues And the two extra coordination positions allow the Tuning of their properties.[1–4] in particular, multiple action ptiv Prodrugs derived from cisplatin have attracted much attention In recent years.[5–7]

On the other hand, cyclometallated ptii compounds containing Bidentate (c,n) or tridentate (c,n,n') ligands display interesting Properties.[8–10] the presence of a s(pt@c) bond increases The stability of these compounds, thus allowing them to Reach the cell unaltered. In addition, covalent coordination to Dna is favoured since the strong pt@c bond increases the lability Of the ligand in a trans position. Moreover, the presence Of aromatic planar groups might favour intercalative binding To dna through noncovalent p–p stacking interactions. Furthermore, Several cyclometallated ptii anticancer agents exhibit Luminescence properties which make them potential luminescent Probes for dna in living cells and also allows easy tracing Of their cellular uptake and distribution by fluorescence microscopy.[11, 12] surprisingly, little attention has been devoted to PtIV compounds containing a metallacycle in spite of their promising properties.[13]

Within the last few years, we have attempted to optimize the ligand design of cyclometallated PtII and PtIV compounds to maximize their efficacy and selectivity against cancer cells.

Indeed, the present work represents a definitive milestone for the optimization of the general formulae [PtX(C,N,N')] and [PtXYZ(C,N,N')], respectively, in which (C,N,N') is a terdentate ligand and X, Y, Z are different ligands such as halido or Cdonor ligands.[14, 15, 16] An additional interesting feature of these (C,N,N')-cycloplatinated compounds relies on their luminescence properties since we have unveiled that the intensity and the energy of the emission can be easily modulated by altering the nature of the ligands, the size of the (N,N')-chelate ring and the substituents in the aryl ring.[17, 18] Indeed, this property of the reported compounds can also be of remarkable interest for in vivo cell imaging and flow cytometry applications.

The syntheses of the (C,N,N') cyclometallated Pt compounds studied in this work are summarised in Scheme 1. These compounds differ in the oxidation state of Pt (II or IV), the length of the hydrocarbyl chain connecting both nitrogen donor atoms (ethylene or propylene), and the halido ligands (Cl or Br).

The new compounds 2b', 3a' and 3b' were characterised by elemental analyses, mass spectra, and 1H and 19F NMR spectra and the molecular structures of these compounds and the previously reported compound 2a' were determined by XRD analysis of suitable crystals (see Figure 1, S1–S7, Supporting Information). In compounds 2a' and 2b' the PtII central atom adopts a square-planar coordination completed with a tridentate (C,N,N') ligand and an halido (Cl for 2a or Br for 2a') ligand trans to the imine. Both the platinacycle and the chelate rings are nearly coplanar with the coordination plane leading to more rigid structures than those previously reported for 2a[17] and 2b[18] containing a propylene chain. For compounds 3a' and 3b', the PtIV central atom displays an octahedral coordination with a meridional

tridentate (C,N,N') ligand and three chlorido (3a') or bromido (3b') ligands. The axial ligands form a Cl-Pt-Cl angle of 175.86(8)8 (3a') or a Br-Pt-Br of 173.85(8)8 (3b').

Absorption and emission spectra for all compounds were recorded in 5V10@5m dichloromethane solutions at 298 K. The results are summarized in Table 1.

PtII cyclometallated compounds show several absorption bands in the UV/Visible range (Figure S8, Supporting Information). The lowest energy bands in the 357–386 nm range can be attributed to Pt(5d)!p* metal-to-ligand charge transfer (MLCT) mixed with intraligand transitions. An additional high energy absorption band, observed in the range 275–301 nm with higher e values, can be attributed to p!p* intraligand transitions, as it matches the absorption recorded for the free ligand (Figure S9, Supporting Information).[18–20] PtIV compounds only show absorption bands in the high energy range, except for compound 3b' which also displays lower energy absorption bands.

When excited at their high energy absorption band, all compounds display a broad emission in the 344–351 nm range assigned as intraligand (1IL) transitions, perturbed by the presence of Pt in the case of the metal complexes (Figure S10, Supporting Information). Trends observed for PtII compounds, indicate that higher luminescent quantum yields are recorded for the more rigid compounds, containing a two carbon hydrocarbyl moiety (2a'>2a and 2b'>2b) and for chlorido derivatives (2a>2b and 2a'>2b'). Although no clear trends are observed for PtIV compounds, the higher quantum yield is obtained for compound 3a' containing chlorido ligands and the more rigid ethylene fragment. PtII complexes and compound 3b' also display a vibronically structured emission band in the 576–630 nm range when excited at their lower energy absorption band (Figure 2). It can be attributed to phosphorescence 3IL emission due to the observation of a large Stokes' shift and the quenching of the emission in the presence of oxygen (Figure S11, Supporting Information).[17, 18]

The stability of the PtIV compound 3a in the aqueous biological medium was evaluated by 1H NMR spectroscopy in D2O and two drops of [D6]DMSO. The obtained spectra (Figure S12, Supporting Information) suggests the formation of a mixture of solvato complexes, which is in line with recent observations of aquation of equatorial ligands of PtIV compounds.[21]

First, we assessed the effect of the PtII and PtIV compounds on the proliferation of a cancer panel including SW620 (lymph node metastasis of colorectal cancer), PC-3 (bone metastasis of prostate cancer), A549 (lung adenocarcinoma), and MCF-7 (breast adenocarcinoma). Our results, summarized in Table 2, indicate that the IC50 of all the compounds except 2a' and 2b' were significantly lower than both cisplatin and oxaliplatin for the breast cancer cell line MCF-7. Also, some of the PtIV compounds displayed IC50 values in the high nanomolar range for SW620 and PC-3. Compound 3a' was the most effective against SW620 (0.41 mm), whereas 3a exhibited the highest efficacy against PC-3 (0.9 mm), A549 (1.4 mm) and MCF-7 (3.3 mm).

We next aimed to evaluate whether these compounds could also be effective against metastatic tumours that have acquired multiplatinum resistance (MPR), for prostate PC-3-MPR and colorectal SW620-MPR, along with their age-matched controls, PC-3O or SW620-O (Tables 3 and 4 and see the

Supporting Information). Strikingly, we obseved that 3a–b' exhibited similar antiproliferative effects in controls and resistant cells of both metastatic resistant cell models, with resistance indexes (RIresist) close to 1, denoting a complete absence of cross-resistance. Indeed, other examples of low cross-resistance have been reported in the literature.[5, 22, 7] However, in such cases, the low cross-resistance is related to the axial ligands, bioactive agents per se (i.e. HDAC, COX, or PDK inhibitors). On the contrary, in our case the absence of cross-resistance must arise from the platinacycle itself, since the axial ligands are halogen groups. In support of this notion, a similar cross-resistance was observed for the PtII structure 2a. Encouragingly, we also found that 2a, 3a, and 3a' displayed excellent selectivity profiles for cancer cells at low doses (1–10 mm), when assessing their antiproliferative effect on all the cancer cell lines tested compared to normal human foreskin fibroblast cells (BJ) (Figures S13–S14, Supporting Information).

In light of these results, we also investigated if the ability to overcome resistance of the reported compounds involved an alteration of their cytotoxic and cytostatic activities inside the cell compared to cisplatin. For that, we studied the effect of 3a' on the cell cycle phase distribution (Figure 3) and apoptosis (Figure 4) of SW620-O and SW620-MPR cells.

We found that, compared to cisplatin, 3a' had only a slight effect on the cell cycle phase distribution of SW620-O cells (Figure 3A). Moreover, whereas cisplatin appeared to induce a significant G2/M arrest, consistent with previous observations,[23] 3a' only occasioned a minor reorganization between the S and G2/M subpopulations, with no effect on the percentage of cells at G0/G1. Indeed, while cisplatin caused a 40% reduction in the G0/G1 subpopulation in SW620-O, it only caused a G0/G1 drop of around 15% in SW620-MPR cells (Figure 3B), with a subsequent G2/M arrest. Interestingly, 3a' had no significant effect on the cell cycle of SW620-MPR cells. On the contrary, 3a' exhibited a much greater effect on the induction of cell death (PI+ cells) than cisplatin in both SW620-O and SW620-MPR (Figure 4). Preapoptotic cells (PI@/Annexin V+ cells) were only observed in SW620-O at 72 h, and both compounds had a significantly enhanced effect on SW620-O than in SW620-MPR cells, potentially denoting that the generated resistant cell lines enhanced their potential to evade apoptosis. In this regard, apoptosis levels did not correlate with ROS accumulation in the cells treated with either cisplatin or 3a' (see Figure S15, Supporting Information).

Previous evidence gathered by our group on different related sets of cyclometallated PtII and PtIV complexes extensively revealed that cellular accumulation for all platinum cyclometallated compounds was significantly higher than for cisplatin.[24, 25] However, no correlation was observed between the cytotoxicity in cancer cells and Pt accumulation within the series of compounds, as previously reported for other metal complexes.[26, 27] Therefore, more information than just intracellular drug concentration, such as reduction potential or differential DNA binding affinity is necessary to explain the displayed enhanced cytotoxicity.

In consequence, the ability of cyclometallated PtII (2a,b, 2a',b') and PtIV (3a,b, 3a',b') compounds to modify the mobility of the supercoiled closed (sc) and the open circular (oc) forms of pBluescript SK+ plasmid DNA was studied in an agarose gel by electrophoresis (Figure 5). For the PtII

complexes significant changes in the mobility of plasmid DNA were observed at 10 mm and even at 5 mm concentration for compounds 2a' and 2b'. With regard to PtIV compounds only 3b' showed an interaction with plasmid DNA at concentrations as high as 100 mm, whereas compounds 3a, 3b and, 3a' were not efficient at all in removing the supercoils from DNA.

Since it is generally accepted that PtIV compounds are rapidly reduced under physiological conditions by cellular reducing agents, the reactions of 3a with ascorbic acid, glutathione, and cysteine were also monitored by 1H NMR spectroscopy under analogous conditions (Figures S16–S18, Supporting Information). The reaction with cysteine (Figure S18) was the most conclusive since it produced from the early stages a compound that is stable in solution for up to one week and that can be assigned to PtII compound 2a–cys (see Scheme S1, Supporting Information). This result is supported by recent studies suggesting that cysteine has the highest reactivity toward reduction of PtIV anticancer prodrugs under physiological conditions and its reactivity is highly sensitive to pH.[28, 29] Additionally, this result is also in agreement with the kinetics studies previously carried out for 3a and analogous $PtIVCl_3$ compounds[30] which revealed that the reaction of these cyclometallated PtIV compounds with thiols consists of two consecutive reaction steps: a PtIV to PtII reduction (step 1 in Scheme S1, Supporting Information) followed by substitution of the remaining chlorido ligand by cysteine (step 2).

In light of this, we hypothesized if the studied Pt compounds could be inhibitors of cysteine metalloprotease Cathepsin B, as recently reported for other metal compounds,[24, 25, 31] but none of the compounds in this study presented significant inhibitory activity.

To evaluate the ability of the PtII and PtIV compounds under study to intercalate with DNA and block the action of topoisomerases, topoisomerase I- and topoisomerase-IIa-based gel assays were also performed.[32] We found that none of the compounds are intercalators or topoisomerase I inhibitors (see Figure S19, Supporting Information). On the contrary, at 50 mm concentration, topoisomerase-IIa inhibition was detected for compounds 2a', 2b', 3a', 3b, and 3b' (see Figure S20, Supporting Information).

In summary, we have presented a new family of luminescent PtII and PtIV (C,N,N')-cycloplatinated compounds with high efficacy and selectivity against a broad cancer cell panel. The studied PtIV compounds presented enhanced efficacy, capacity to be reduced in solution and, importantly, a complete absence of platinum cross-resistance against metastatic CRC and CRPC multiplatinum-resistant cell models. Indeed, we also proved that the absence of cross-resistance is an intrinsic property of the platinacycle. Therefore, further modulating the nature of the axial ligands could allow us to remarkably improve the multitarget action of the compounds, leading to unparalleled levels of efficacy and to ultimately overcome platinum resistance in the clinics.

ACKNOWLEDGEMENTS

This work was supported by the Ministerio de Economia y Competitividad (Projects CTQ-2015–65040-P, CTQ2015-65707C2-1/FEDER, AEI/FEDER CTQ2016-76120-P, CTQ2017-90802-REDT, SAF2017-89673-R and SAF2015-70270-REDT), Instituto de Salud Carlos III and Centro de Investigacijn Biom8dica en Red de Enfermedades Hep#ticas y Digestivas (CIBEREHD CB17/04/00023), AgHncia de Gestij d'Ajuts Universitaris i de Recerca (AGAUR)—Generalitat de Catalunya (2017SGR-1033).

M. Cascante acknowledges the support received through the prize "ICREA Academia" for excellence in research, funded by ICREA foundation—Generalitat de Catalunya.

REFERENCES

[1] T. C. Johnstone, K. Suntharalingam, S. J. Lippard, Chem. Rev. 2016, 116, 3436–3486.

[2] R. G. Kenny, W. Chuah, A. Crawford, C. J. Marmion, Eur. J. Inorg. Chem. 2017, 1596–1612.

[3] Z. Wang, Z. Deng, G. Zhu, Dalton Trans. 2019, 48, 2536–2544.

[4] D. Gibson, J. Inorg. Biochem. 2019, 191, 77–84.

[5] E. Petruzzella, R. Sirota, I. Solazzo, V. Gandin, D. Gibson, Chem. Sci. 2018, 9, 4299–4307.

[6] R. G. Kenny, C. J. Marmion, Chem. Rev. 2019, 119, 1058–1137.

[7] H. Kostrhunova, E. Petruzzella, D. Gibson, J. Kasparkova, V. Brabec, Chem. Eur. J. 2019, 25, 5235–5245.

[8] N. Cutillas, G. S. Yellol, C. De Haro, C. Vicente, V. Rodr&guez, J. Ruiz, Coord. Chem. Rev. 2013, 257, 2784–2797.

[9] I. Omae, Coord. Chem. Rev. 2014, 280, 84–95.

[10] M. Clemente, I. H. Polat, J. Albert, R. Bosque, M. Crespo, J. Granell, C. Ljpez, M. Mart&nez, J. Quirante, R. Messeguer, C. Calvis, J. Badia, L. Baldom /, M. Font-Bardia, M. Cascante, Organometallics 2018, 37, 3502 – 3514.

[11] Y. Zhang, Q. Luo, W. Zheng, Z. Wang, Y. Lin, E. Zhang, S. Le, J. Xiang, Y. Zhao, F. Wang, Inorg. Chem. Front. 2018, 5, 413–424.

[12] T. Zou, J. Liu, C. T. Lum, C. Ma, R. C. T. Chan, C. N. Lok, W. M. Kwok, C. M. Che, Angew. Chem. Int. Ed. 2014, 53, 10119–10123; Angew. Chem. 2014, 126, 10283–10287.

[13] M. Crespo, J. Organomet. Chem. 2019, 879, 15–26.

[14] A. Escol/, M. Crespo, J. Quirante, R. Cort8s, A. Jayaraman, J. Badia, L. Baldoma, T.. Calvet, M. Font-Bardia, M. Cascante, Organometallics 2014, 33, 1740–1750.

[15] E. Bauer, X. Domingo, C. Balcells, I. H. Polat, M. Crespo, J. Quirante, J. Bad&a, L. Baldom/, M. Font-Bardia, M. Cascante, Dalton Trans. 2017, 46, 14973–14987.

[16] M. Sol8, C. Balcells, M. Crespo, J. Quirante, J. Badia, L. Baldom/, M. Font-Bardia, M. Cascante, Dalton Trans. 2018, 47, 8956–8971.

[17] A. Gandioso, J. Valle-Sistac, L. Rodr&guez, M. Crespo, M. Font-Bard&a, Organometallics 2014, 33, 561–570.

[18] A. L#zaro, O. Serra, L. Rodr&guez, M. Crespo, M. Font-Bardia, New J. Chem. 2019, 43, 1247–1256.

[19] G. Mill#n, N. Gim8nez, R. Lara, J. R. Berenguer, M. T. Moreno, E. Lalinde, E. Alfaro-Arnedo, I. P. Ljpez, S. Pineiro-Hermida, J. G. Pichel, Inorg. Chem. 2019, 58, 1657–1673.

[20] C. Song, J. Tang, J. Li, Z. Wang, P. Li, H. Zhang, Inorg. Chem. 2018, 57, 12174–12186.

[21] A. Kastner, I. Poetsch, J. Mayr, J. V. Burda, A. Roller, P. Heffeter, B. K. Keppler, C. R. Kowol, Angew. Chem. Int. Ed. 2019, 58, 7464–7469; Angew. Chem. 2019, 131, 7542–7547.

[22] E. Petruzzella, J. P. Braude, J. R. Aldrich-Wright, V. Gandin, D. Gibson, Angew. Chem. Int. Ed. 2017, 56, 11539–11544; Angew. Chem. 2017, 129, 11697–11702.

[23] N. Sarin, F. Engel, G. V. Kalayda, M. Mannewitz, J. Cinatl, F. Rothweiler, M. Michaelis, H. Saafan, C. A. Ritter, U. Jaehde, R. Frçtschl, PLoS One 2017, 12, e0181081.

[24] A. Escol/, M. Crespo, C. Ljpez, J. Quirante, A. Jayaraman, I. H. Polat, J. Bad&a, L. Baldom/, M. Cascante, Bioorg. Med. Chem. 2016, 24, 5804 – 5815.

[25] J. Albert, R. Bosque, M. Crespo, J. Granell, C. Ljpez, R. Mart&n, A. Gonz #lez, A. Jayaraman, J. Quirante, C. Calvis, J. Badia, L. Baldom/, M. Font-Bardia, M. Cascante, R. Messeguer, Dalton Trans. 2015, 44, 13602 – 13614.

[26] J. Ruiz, C. Vicente, C. De Haro, A. Espinosa, Inorg. Chem. 2011, 50, 2151 – 2158.

[27] A. C. Komor, J. K. Barton, Chem. Commun. 2013, 49, 3617–3630.

[28] J. Dong, S. Huo, S. Shen, J. Xu, T. Shi, L. I. Elding, Bioorg. Med. Chem. Lett. 2016, 26, 4261–4266.

[29] A. Chipman, B. F. Yates, A. J. Canty, A. Ariafard, Chem. Commun. 2018, 54, 10491–10494.

[30] M. Crespo, M. Font-Bardia, P. Hamidizadeh, M. Mart&nez, S. M. Nabavizadeh, Inorg. Chim. Acta 2019, 486, 8–16.

[31] S. P. Fricker, Metallomics 2010, 2, 366–377.

[32] J. Albert, R. Bosque, M. Cadena, L. D'Andrea, J. Granell, A. Gonz#lez, J. Quirante, C. Calvis, R. Messeguer, J. Badia, L. Baldom/, T. Calvet, M. Font-Bardia, Organometallics 2014, 33, 2862–2873.

Legends to figures

Scheme 1. Synthesis of cyclometallated PtII and PtIV compounds. (i)+ cis-[PtCl2(DMSO)2] and Na(CH3COO), methanol, reflux, 72 h; (ii)+ KBr, methanol, reflux, 48 h; (iii)+ PhICl2, acetone, r.t., 1 h; (iv)+ Br2, acetone, r.t., 1 h.

Figure 1. Molecular structure of compound 3a'. Selected bond lengths [a] and angles [8] with estimated standard deviations: Pt(1)@N(8): 1.984(8); Pt(1)@N(11): 2.253(8); Pt(1)@C(1): 2.019(9); Pt(1)@Cl(1): 2.320(2); Pt(1)@Cl(2): 2.313(2); Pt(1)@Cl(3): 2.322(2); C(1)-Pt-N(8): 81.6(3); N(8)-Pt-N(11): 82.2(3); N(11)-Pt-Cl(1): 97.8(2); Cl(1)-Pt-C(1): 98.4(3); Cl(2)-Pt-Cl(1): 90.02(8); Cl(2)-Pt-N(8): 90.6(2) ; Cl(2)-Pt-N(11): 90.0(2); Cl(2)-Pt-C(1): 87.0(3); Cl(3)-Pt-Cl(1): 90.78(8); Cl(3)-Pt-N(8): 88.6(2); Cl(3)-Pt-N(11): 93.9(2); Cl(3)-Pt-C(1): 88.8(3).

Figure 2. Normalized emission spectra of the Pt compounds in dichloromethanesolution at 298 K. lexc (nm)=385 (2a'), 385 (2b'), 380 (3b').

Figure 3. Cell cycle phase distribution at 72 h incubation with cisplatin or 3a' at their IC50 concentration in (A) SW620-O and (B) SW620-MPR.

Figure 4. Percentage variations of alive, early apoptotic and late apopto- tic/necrotic cell populations at 72 h incubation with cisplatin or 3a' at their IC50 concentrations in (A) SW620-O and (B) SW620-MPR cells.

Figure 5. Interaction of pBluescript SK+ plasmid DNA (0.3 mg) with increasing concentrations of compounds under study. A) All compounds were analysed from 10 to 200 mm concentration Lane 1: DNA only. Lane 5: 10 mm. Lane 6: 25 mm. Lane 7: 50 mm. Lane 8: 100 mm. Lane 9: 200 mm. B) Compound 2a' and 2b' were also analysed at lower concentrations and compared with cisplatin as a standard reference. Lane 1: 0 mm. Lane 2: 1 mm. Lane 3: 2.5 mm. Lane 4: 5 mm. Lane 5: 10 mm. Lane 6: 25 mm. Lane 7: 50 mm. Lane 8: 100 mm. Lane 9: 200 mm; sc=supercoiled closed circular DNA; oc=open circular DNA.

SCHEME 1.

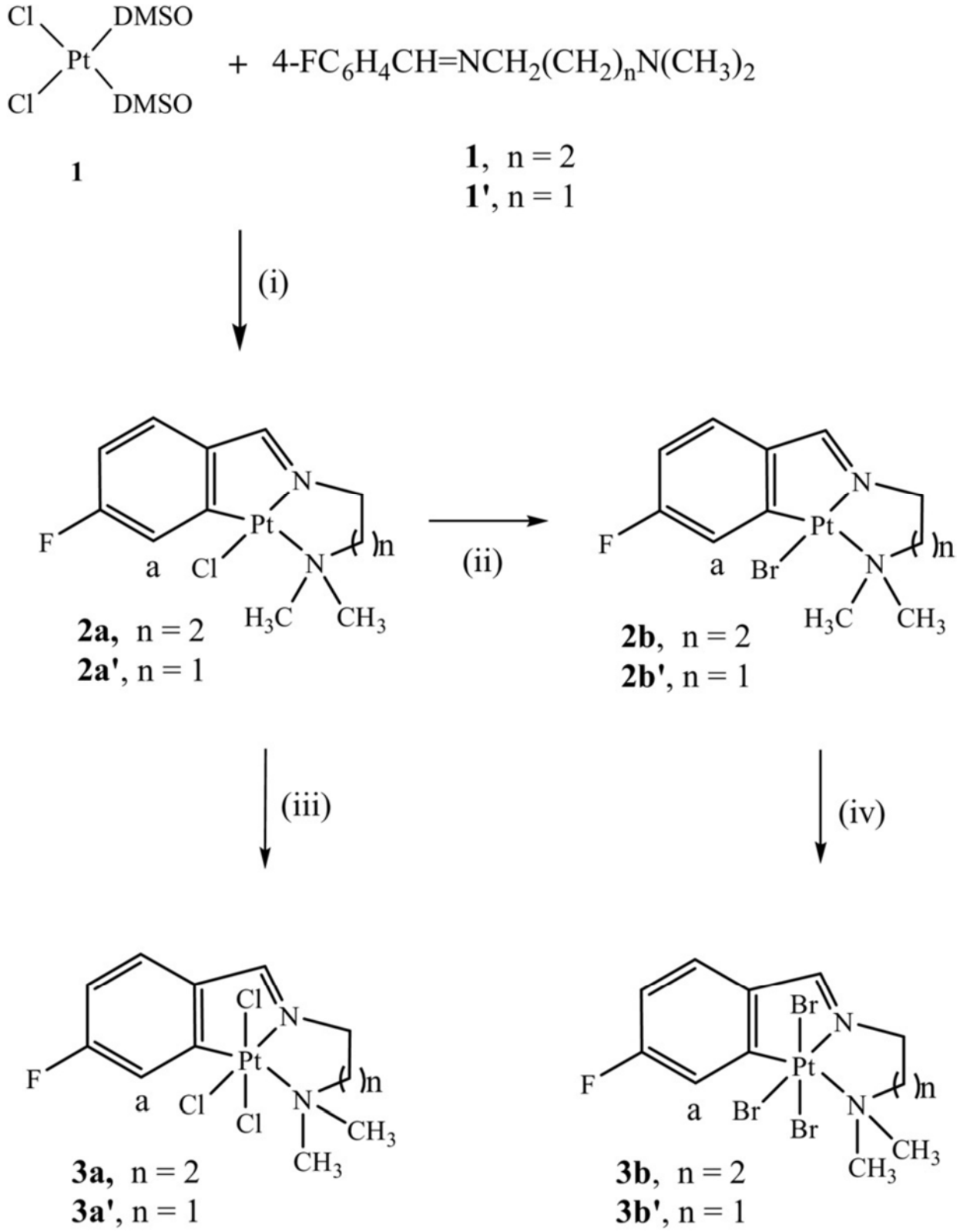
Cl
DMSO
Pt
Cl
DMSO
+ 4-FC6H4CH=NCH2(CH2)nN(CH3)2
1
1, n = 2
1', n = 1
(i)
F
a
Cl
Pt
N
n
H3C
CH3
2a, n = 2
2a', n = 1
(ii)
Br
2b, n = 2
2b', n = 1
(iii)
(iv)
3a, n = 2
3a', n = 1
3b, n = 2
3b', n = 1

FIGURE 1

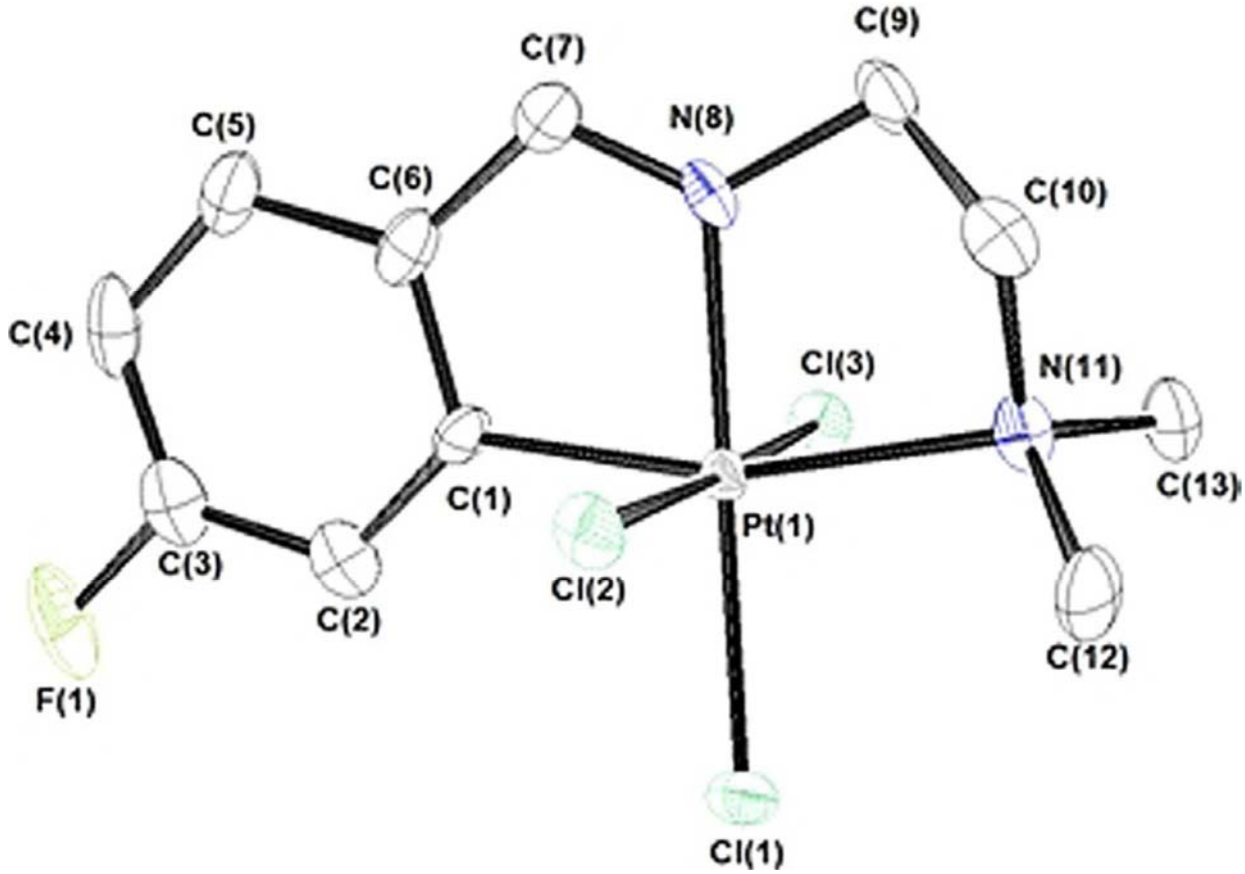

323 **FIGURE** 2

324

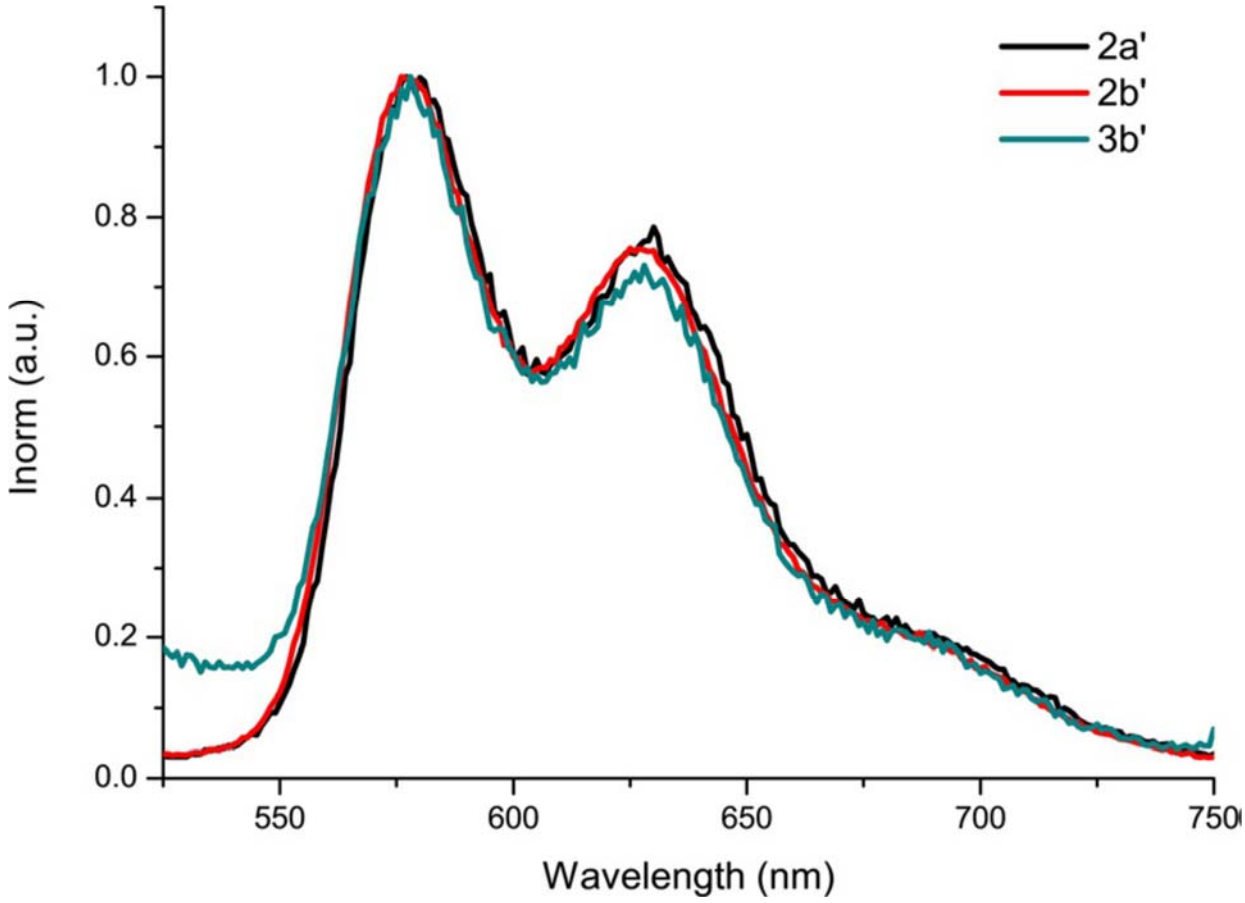

325

326

327

FIGURE 3

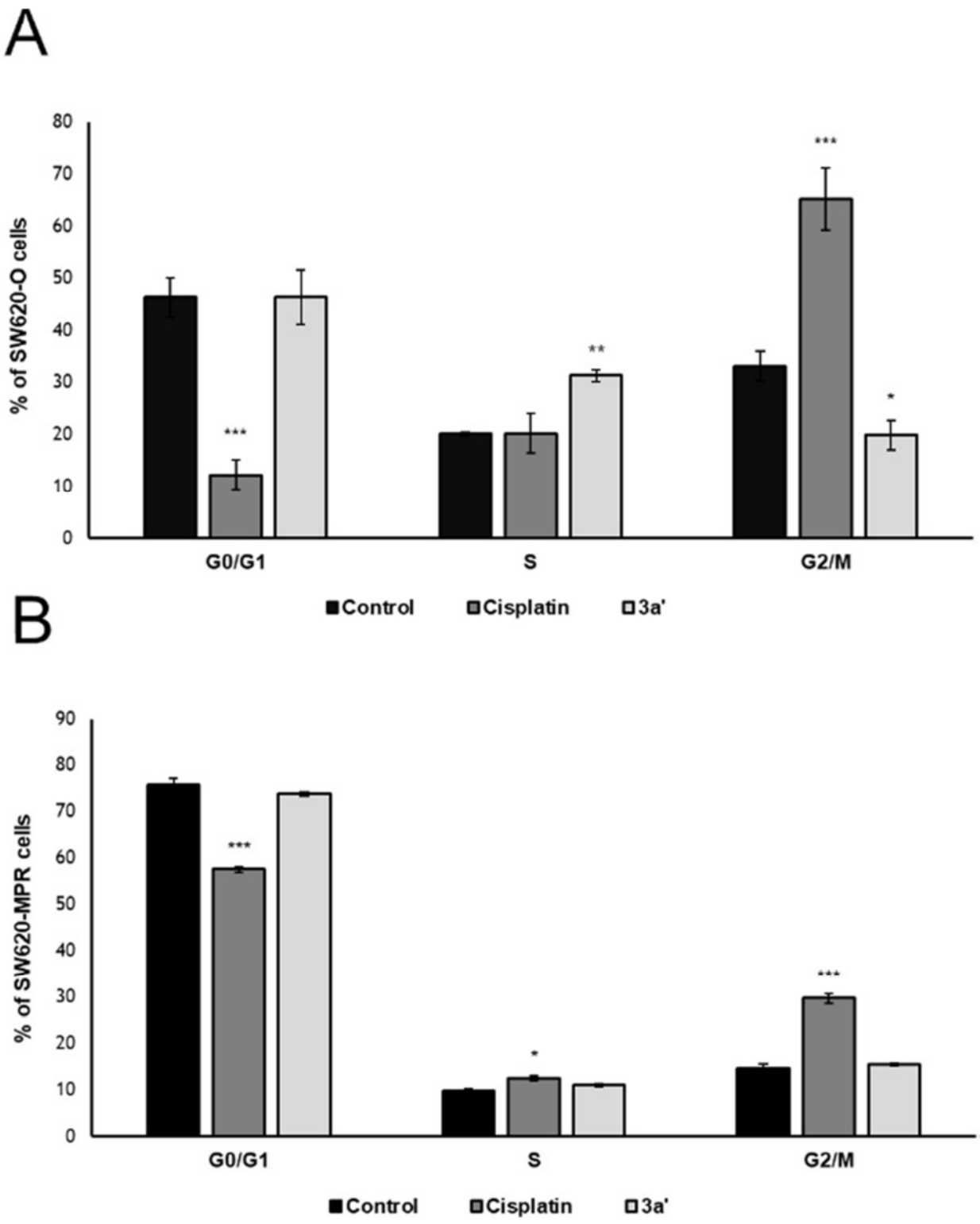
A
% of SW620-O cells
80
70
60
50
40
30
20
10
0
***
**
***
*
G0/G1
S
G2/M
Control
Cisplatin
3a'
B
% of SW620-MPR cells
90
80
70
60
50
40
30
20
10
0
***
*
***
G0/G1
S
G2/M
Control
Cisplatin
3a'

FIGURE 4

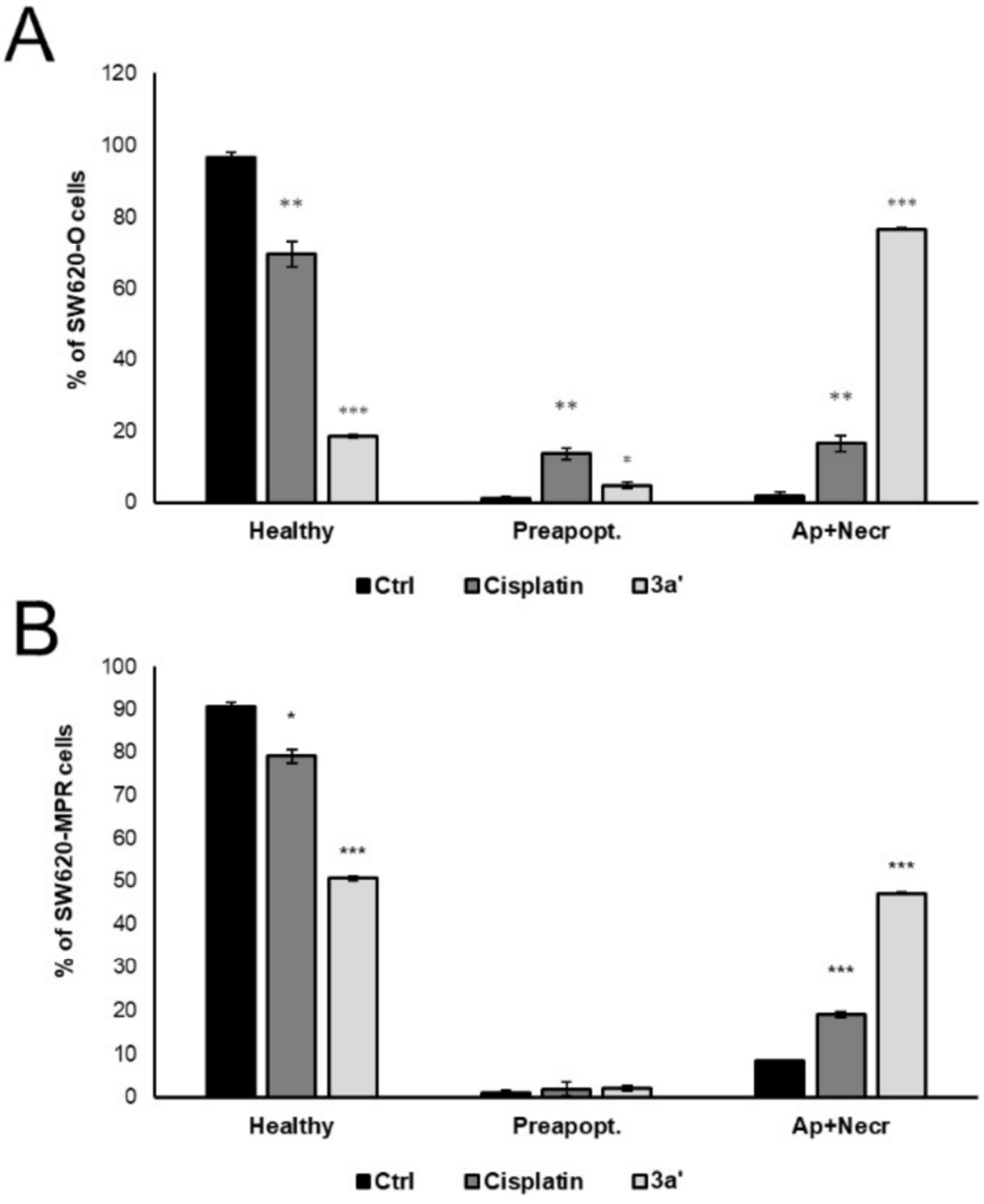
A
120
100
80
60
40
20
0
% of SW620-O cells
**
***
**
*
**
***
Healthy
Preapopt.
Ap+Necr
Ctrl
Cisplatin
3a'
B
100
90
80
70
60
50
40
30
20
10
0
% of SW620-MPR cells
*
***
***
***
Healthy
Preapopt.
Ap+Necr
Ctrl
Cisplatin
3a'

FIGURE 5

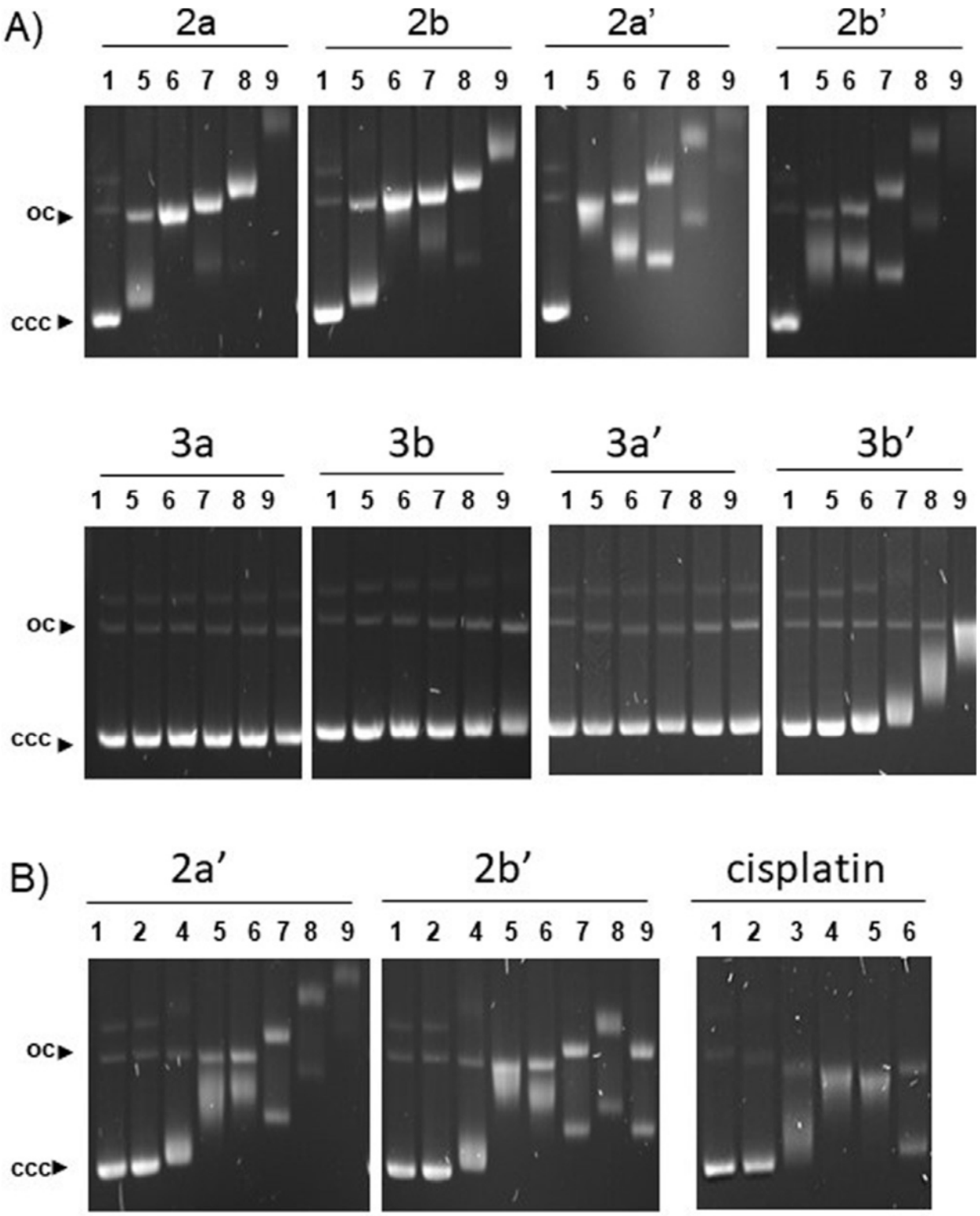
A)
2a
2b
2a'
2b'
1 5 6 7 8 9
oc
ccc
3a
3b
3a'
3b'
B)
2a'
2b'
cisplatin
1 2 4 5 6 7 8 9
1 2 3 4 5 6

Table 1. Absorption and emission data for compounds **1**, **2** and **3** in dichloromethane solution at 298 K

Compd.	Absorption λ_{max} [nm] (ε [M^{-1} cm^{-1}])	Emission λ_{max} [nm]	Φ
1[18]	276 (1506), 286 (1060)	350	0.074[a]
1′	275 (1994), 286 (1295)	346	0.059[a]
2a[14]	285 (3443), 311 (2563),	347	0.056[a]
	357 (2387), 374 (2618)	577, 620	0.003[b]
2b[16]	288 (4524), 318 (2713)	349	0.044[a]
	357 (2140), 378 (2618)	576, 622	0.004[b]
2a[17]	277 (7524), 288 (5960)	344	0.069[a]
	324 (4843), 383 (4203)	577, 630	0.005[b]
2b′	280 (7645), 291 (6901)	350	0.065[a]
	326 (5898), 386 (5396)	576, 625	0.006[b]
3a[14]	287 (3831)	349	0.051[a]
3b[16]	286 (6353)	350	0.056[a]
3a′	270 (22 702), 336 (2655)	352	0.123[a]
3b′	280 (12 290), 301 (9805)	351	0.046[a]
	340 (4097), 380 (2228)	578, 628	0.002[b]

[a] Quantum yields for emission in solution referred to naphthalene in cyclohexane. [b] Quantum yields for emission in solution referred to $[Ru(bipy)_3]Cl_2$ in H_2O.

Table 2. Antiproliferative activity (IC_{50}, μM) on A549 lung, SW620 colorectal, MCF-7 breast and PC-3 prostate cancer cell lines for the studied compounds, cisplatin and oxaliplatin.

Compd.[a]	A549	SW620	MCF-7	PC-3
2a	5±2	5.7±1.1	6±2	1.1±0.6
2b	5±2	5.5±0.4	7±2	2.1±1.3
2a′	57±3	4.6±0.8	>100	19±5
2b′	48±5	3.1±1.1	>100	66±13
3a	1.4±0.5	0.9±0.3	3.3±0.5	0.9±0.2
3b	3.39±0.12	1.8±0.7	6.6±0.8	1.46±0.13
3a′	4.1±0.3	0.41±0.04	5.4±1.0	1.2±0.5
3b′	4±2	0.7±0.4	8.0±0.8	1.46±0.11
Cisplatin[b]	5.5±0.2	1.4±0.5	25.6±0.7	1.5±0.4
Oxaliplatin[b]	1.3±0.2	0.3±0.2	23.4±0.2	1.2±0.3

[a] Results shown correspond to mean ± standard deviation of two experiments performed in triplicates. [b] Cisplatin and oxaliplatin are taken as reference compounds.

Table 3. Antiproliferative activity (IC_{50}, μM) and resistance index (RI) of the studied compounds, cisplatin and oxaliplatin on the generated colorectal cancer (CRC) model of multiplatinum resistance (SW620-MPR) and its age-matched control (SW620-O).

Compd.[a]	SW620-O	SW620-MPR	RI_{aging}[b]	RI_{resist}[c]	RI_{total}[d]
2a	7±3	7.1±0.6	1	**1**	1.3
3a	2.2±0.3	3±2	2.4	**1.2**	2.8
3b	3.6±1.2	4.8±1.4	2	**1.3**	2.7
3a′	1.1±0.7	1.64±0.01	2.8	**1.4**	4
3b′	0.8±0.4	1.4±0.7	1.2	**1.7**	2
Cisplatin	1.1±0.9	21±4	0.8	**19**	15
Oxaliplatin	0.3±0.2	3.2±1.1	1	**10**	10

[a] Results shown correspond to mean ± standard deviation of two experiments performed in triplicates. [b] RI_{aging} corresponds to the ratio of IC50 between SW620-O (age-matched control) and SW620 (parental). [c] RI_{resist} corresponds to the ratio of IC50 between SW620-MPR (resistant) and SW620-O (age-matched control). [d] RI_{total} corresponds to the ratio of IC50 between SW620-MPR (resistant) SW620 (parental).

Table 4. Antiproliferative activity (IC_{50}, μM) and resistance index (*RI*) of the studied compounds, cisplatin and oxaliplatin on the generated castration-resistant prostate cancer (CRPC) model of multiplatinum resistance (PC-3-MPR) and its age-matched control (PC-3-O).

Compound[a]	PC-3-O	PC-3-MPR	RI_{aging}[b]	RI_{resist}[c]	RI_{total}[d]
2a	0.67 ± 0.11	1.6 ± 0.2	0.6	**2.5**	1.5
3a	1.4 ± 0.8	1.5 ± 0.3	1.5	**1**	1.6
3b	5.3 ± 0.3	3.7 ± 1.3	3.7	**0.7**	2.5
3a′	2 ± 2	2.9 ± 0.4	1.9	**1.3**	2.4
3b′	4 ± 2	3.7 ± 0.4	2.4	**1**	2.5
Cisplatin	2.5 ± 0.9	23 ± 9	1.7	**9**	15
Oxaliplatin	0.69 ± 0.02	51 ± 12	0.6	**74**	42

[a] Results shown correspond to mean ± standard deviation of two experiments performed in triplicates. [b] RI_{aging} corresponds to the ratio of IC_{50} between PC-3-O (age-matched control) and PC-3 (parental). [c] RI_{resist} corresponds to the ratio of IC_{50} between PC-3-MPR (resistant) and PC-3-O (age-matched control). [d] RI_{total} corresponds to the ratio of IC_{50} between PC-3-MPR (resistant) and PC-3 (parental).